TECTONICS, VOL. 6, NO. 5, PAGES 653-666, OCTOBER 1987

# DEFORMATION ALONG THE YAMMUNEH, THE RESTRAINING BEND OF THE DEAD SEA TRANSFORM: PALEOMAGNETIC DATA AND KINEMATIC IMPLICATIONS

Hagai Ron[1]

Department of Geophysics, Stanford University, Stanford, California

Abstract. A simple geometrical model shows that the plate margin along the restraining bend segment of the transform plate boundary be deformed in order to accommodate overlap of the crust. This model predicts both the maximum width of the deformed zone and the magnitude of deformation when the general geometry of the plate margin is known as well as the plate slip vector and the amount of cumulative displacement. This idea has been tested along the plate margin of the Yammuneh restraining bend of the Dead Sea transform. The plate margin has been deformed by NNE folding parallel to the restraining bend and by east-west trending, right-lateral strike-slip faults. Paleomagnetic measurements yield counterclockwise rotation of $R \pm \Delta R = 61.0° \pm 9.6°$ and $F \pm \Delta F = 23.4° \pm 17.2°$. The paleomagnetic rotational data and fault kinematic suggest that the mechanism which accommodates regional left-lateral shear is simultaneous right-lateral strike-slip faulting on secondary faults and block rotation. The magnitude of deformation is the same as that predicted by the model, which is 100% shortening in a direction parallel to the plate slip vector and negligible deformation in a direction parallel to the transform. The large amount of rotation implies that probably more than one fault set is involved and present day seismic activity is the current manifestation of this crustal deformation process. If this prediction is correct, then the current deformation of the plate margin is accommodated by more favorable newly formed NNW right-lateral strike-slip faults.

## INTRODUCTION

The en echelon geometry and restraining bend segment are common geometrical features of strike-slip and transform faults, such as the San Andreas (California) and the Alpine (New Zealand) faults and the Dead Sea (Levant) transform, to name only a few. Continuous slip along wrench faults typically results in pull-aparts or pressure ridges in areas of relative extension or compression, respectively. The type of deformation is thus controlled by the sense of displacement versus the sense of the stepping in en echelon geometry or the sense of bending of the fault. In this paper, by using simple kinematic and geometrical

[1]Now at The Institute for Petroleum Research and Geophysics, Holon, Israel.



Paper number 7T0477.
0278-7407/87/007T-0477$10.00

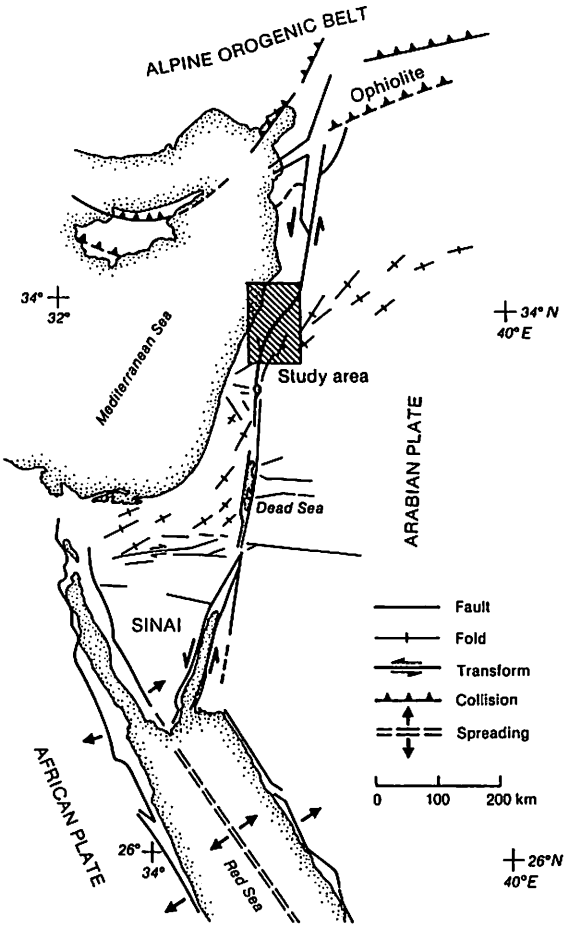


Fig 1. General plate tectonic setting of the Dead Sea transform (modified after Garfunkel [1981]. The age of the Syrian arc fold belt is of Upper Cretaceous to Eocene.

considerations, an attempt has been made to assess the possible mechanism and magnitude of deformation of the plate margin along the restraining bend segment of the Dead Sea transform (Figure 1).

The Dead Sea transform strikes about north-south, whereas its restraining bend segment, the Yammuneh, is striking N30°E. The geometry of the plate boundary (Arabia and Sinai-Israel sub-subplates), when combined with the 105 km of relative left-lateral displacement between the plates, results in a large compressive component along this segment oblique to the plate motion slip vector (Figure 1). If the plates are rigid, geometrical considerations would predict that an overlap between the two plates should develop. Since in the case of the Yammuneh segment, no significant thickening of the crust has been observed [Beydoun, 1977], it might be expected that lateral deformation would take place in order to release the stress and eliminate the overlap (Figure 2). The tectonics of oblique transform which cause transversal shortening can be demonstrated and summarized in a simple model which takes into account the geometry of the plate boundary, the magnitude of relative displacement, and the orientation of the plate slip vector. From this model, which assumes constant geometry through time, the maximum width of both the plate margin deformed zone and the magnitude of deformation relative to the plate slip vector can be established.

From a simple model (Figure 2) it appears that the width (w) of the deformed zone is defined by

$$w = d \sin \beta \qquad (1)$$

where d is the displacement along the major fault and $\beta$ is the angle between the

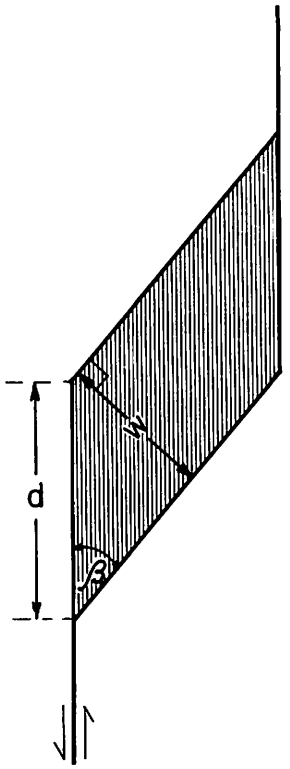


Fig. 2. The geometrical relation between d, the displacement along the fault, $\beta$, the angle between the fault and the fault slip vector, and W, the width of the deformed zone perpendicular to the restraining bend segment (see Figure 1).

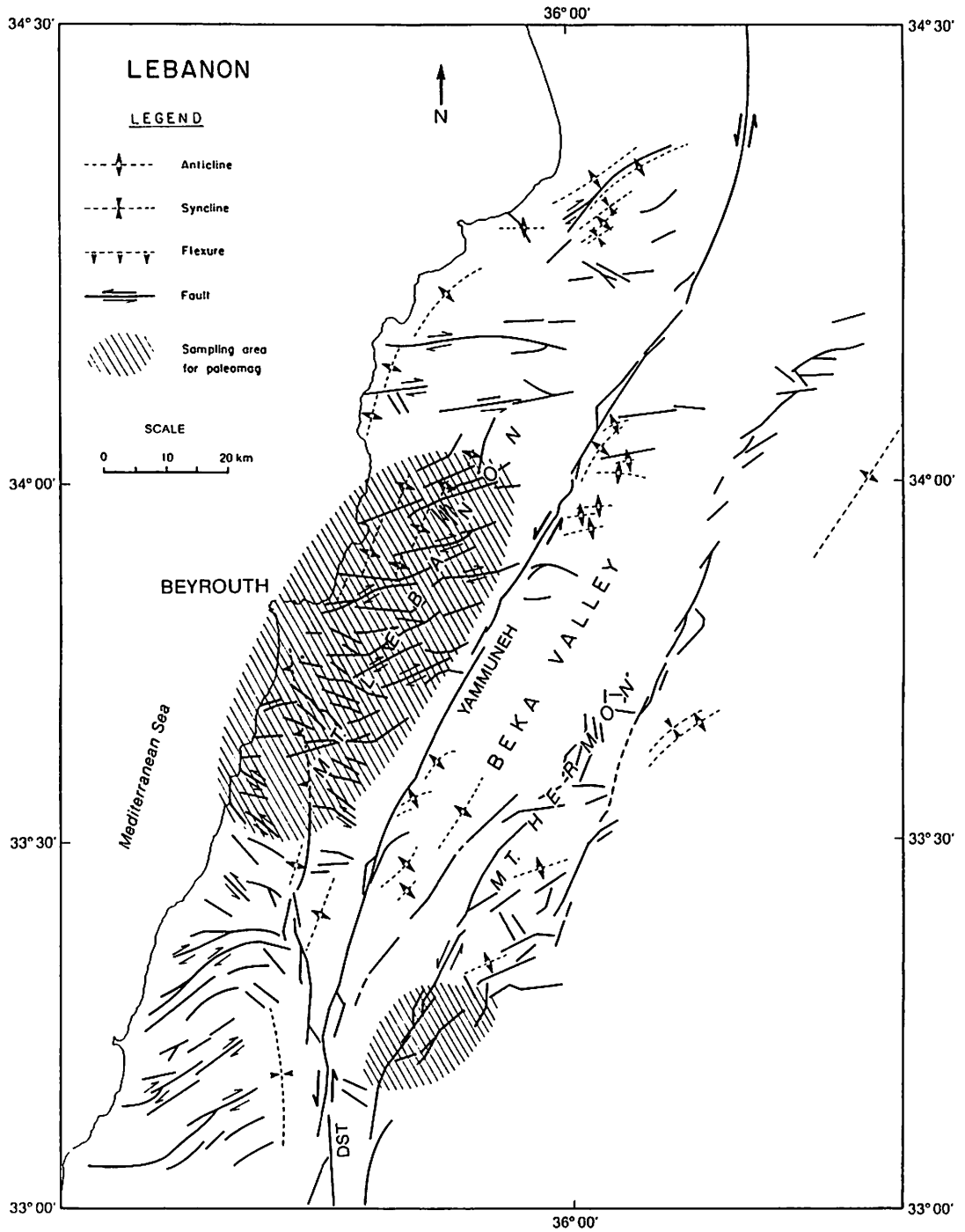


Fig. 3. Faults and folds map of the plate margin next to the Yammuneh bend segment of the Dead Sea transform.

strike of the restraining bend segment and the orientation of the slip vector. In order to avoid overlap between the plates the expected shortening of a line parallel to the plate slip vector should be half its original length. Various models for the deformation between en echelon faults and restraining bend fault segments have been suggested by Freund [1974], Kosloff [1977] and Segall and

TABLE 1. Compilation of Paleomagnetic Data, Mount Hermon

| Site | N | Inc., deg. | Dec., deg. | $\alpha_{95}$° | K | Age, m.y. K-Ar | | Polarity |
|---|---|---|---|---|---|---|---|---|
| 1 | 6 | 1.7 | 290.5 | 10.30 | 31.00 | 114.9 | ±3.8 | N |
| 2 | 8 | -10.2 | 274.5 | 7.50 | 55.44 | | | |
| 3 | 7 | 27.9 | 81.5 | 5.47 | 122.60 | | | |
| 4 | 6 | 18.9 | 86.2 | 8.67 | 60.64 | 118.7 | ±5.3 | R |
| 5 | 7 | 19.8 | 108.6 | 5.51 | 121.15 | | | |
| 6 | 6 | 23.2 | 293.8 | 12.86 | 28.08 | | | |
| 7 | 7 | -9.8 | 270.7 | 9.43 | 41.96 | 113.2 | ±3.8 | N |
| 8 | 6 | 28.9 | 81.0 | 7.90 | 52.03 | | | |
| 9 | 7 | -26.0 | 208.9 | 6.80 | 60.54 | | | |
| 10 | 4 | -60.9 | 113.0 | 1.55 | 2029.00 | | | |
| 11 | 6 | 7.8 | 85.6 | 5.00 | 130.20 | 118.4 | ±1.2 | R |
| 12 | 7 | 17.9 | 271.2 | 4.80 | 120.75 | | | |
| 13 | 6 | 3.9 | 281.4 | 6.00 | 90.20 | | | |

Source: this study. For site location, see Figure 5. N, number of samples; inc., inclination; dec., declination; $\alpha_{95}$, radius of 95% confidence in deg; K, precision parameters; K-Ar, age after More et al. [1984].

Pollard [1980], but these models discuss mainly the stress field rather than the deformation.

In order to test the idea that deformation of the plate margin accommodates and avoids overlap of the plates the paleomagnetism of Cretaceous volcanics and intrusive rocks from Mount Hermon and additional paleomagnetic data from Mount Lebanon [Gregor et al., 1974] were studied. To assess the extent of regional crustal deformation, estimation of the degree of shortening based on a simple kinematic model of rotating blocks has been calculated. The area of investigation is the deformed plate margin of the Dead Sea transform adjacent to the Yammuneh restraining fault bend.

## GENERAL TECTONICS AND STRUCTURE

The tectonic location of Mount Hermon and Lebanon on plate margins of oblique transform [Freund et al., 1970; Hancock and Atyia, 1979; Freund and Tarling, 1979; Garfunkel et al., 1981] give rise to a transpressive regime normal to the boundary (Figure 3). Restoring the 105 km of sinistral displacement should give an overlap of about 55 km. Gravity data [Beydoun, 1977, and reference therein] have been interpreted to indicate very recent uplift of the Lebanon and Mount Hermon ranges, as yet uncompensated isostatically; therefore, both uplifts are lack of roots. Moreover, Tiberghien [1974] calculated the depth to the Moho to be 27 to 28 km below sea level at the coast and 30 to 31 km in the Beka'a, with the crust thickening eastward, which reflects the regional thickening from the Mediterranean inland. Therefore the undetected thickening of the upper brittle crust suggests that deformation of the crust should accommodate the overlap.

The topography of the region is dominated by north-northeast trending mountain ranges (parallel to the transform) of Mount Lebanon and Mount Hermon separated by the Beka'a valley. The ranges reflect anticlinoria, while the Beka'a reflects synclinoria. This structure exposes 3000 m of shallow marine carbonate and sandstone ranging in age from Middle Jurassic to Eocene [Dubertret, 1955; Renouard, 1955; Beydoun, 1977]. The section also includes Upper Jurassic to Lower Cretaceous volcanics and shallow intrusive rocks. These ages are suggested by Dubertret [1955], but according to Beydoun [1977], the age of the volcanic rocks in Lebanon is Lower Cretaceous. A recent study by Mor et al., [1984] using the K-Ar method suggests that these rocks, at least from the Mount Hermon range, are of Lower Cretaceous (Aptian) age (Table 1).

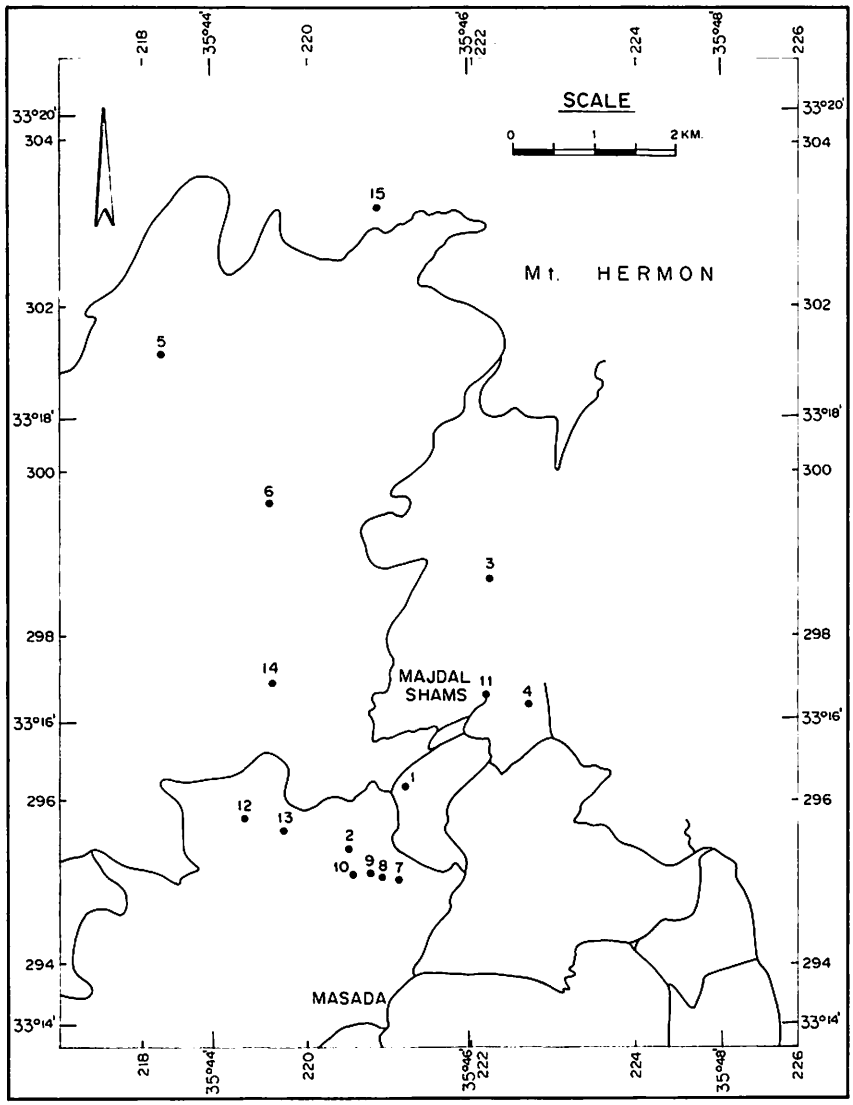


Fig. 4. Location map of paleomagnetic sampling sites in the Mount Hermon region, showing main roads and Israel and international grids.

The dominant structural elements of the region, as described by Dubertret [1955], Renouard [1955], Beydoun [1977], and Hancock and Atyia [1979], are folds and faults (Figure 3). The scale of folding ranges from tens of meters to kilometers and affects rock units from Jurassic to Pliocene (at least). The majority of folds trend north-northeast parallel to the anticlinorium, but to the northwest of the Mount Lebanon range and in the Hermon range they trend northeast. The monoclinal flexure is usually associated with high-angle reverse faults. Conjugate sets of right-lateral faults trending northwest to east-west and left-lateral faults trending north-south to north-northeast are the dominant faulting elements (Figure 3). Hancock and Atyia [1979] suggested that the amount of shortening achieved by folding and faulting rarely exceeds 10% and is less than that which would be anticipated as a consequence of the north-south left-lateral displacement along the Dead Sea transform colliding against the north-northeast trending Yammuneh segment. Freund and Tarling [1979] first suggest that the deformation might be explained by strike-slip faulting and block rotation

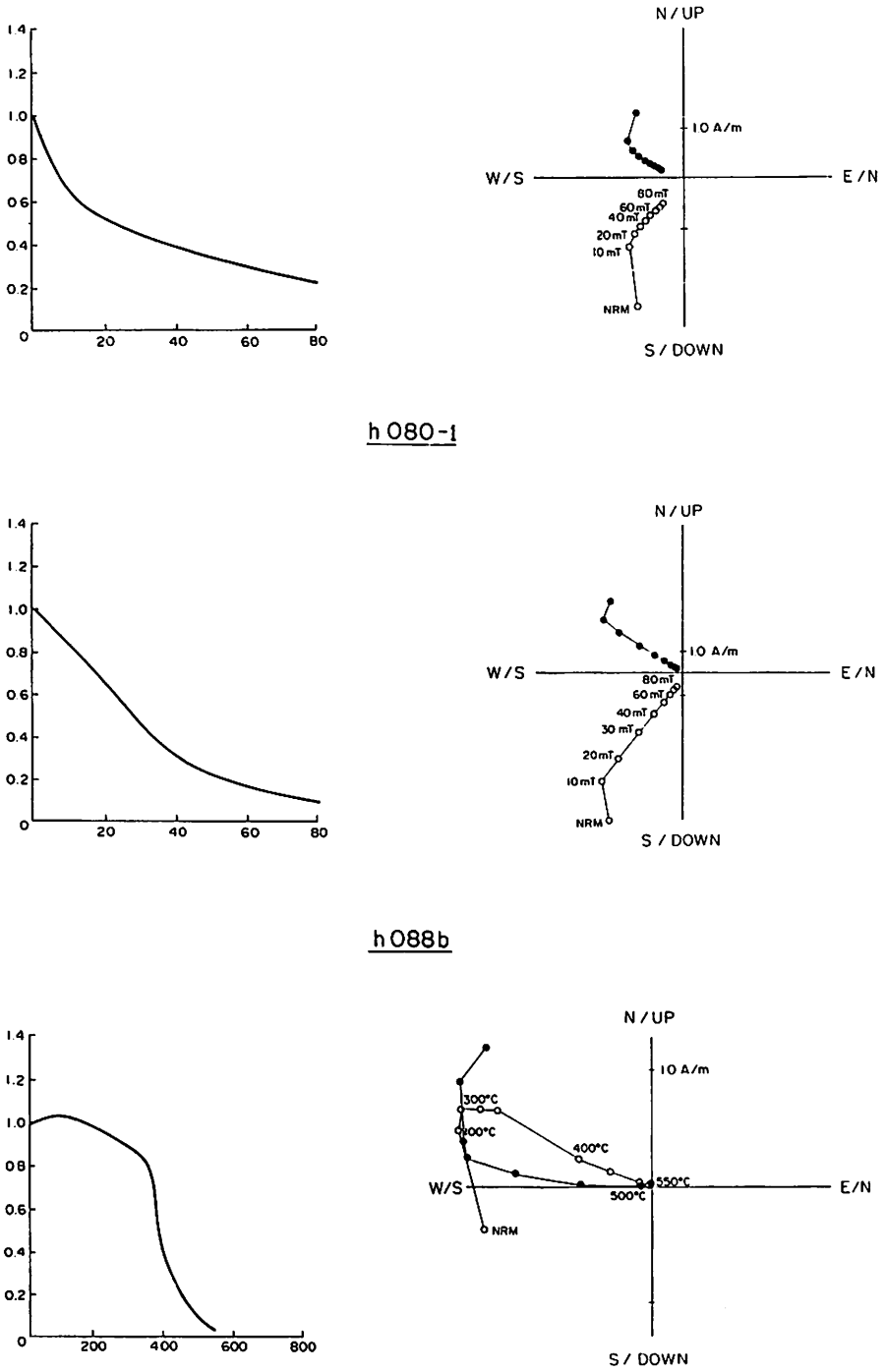


Fig. 5. Orthogonal vector plot and normalized intensity $J/J_0$ for five samples of volcanic rocks, of Hermon region, during stepwise demagnetization. AF values are in milleteslas and temperatures in degrees Celcius. Solid circles represent the north and west or east component and open circles represent the north or south and down component.

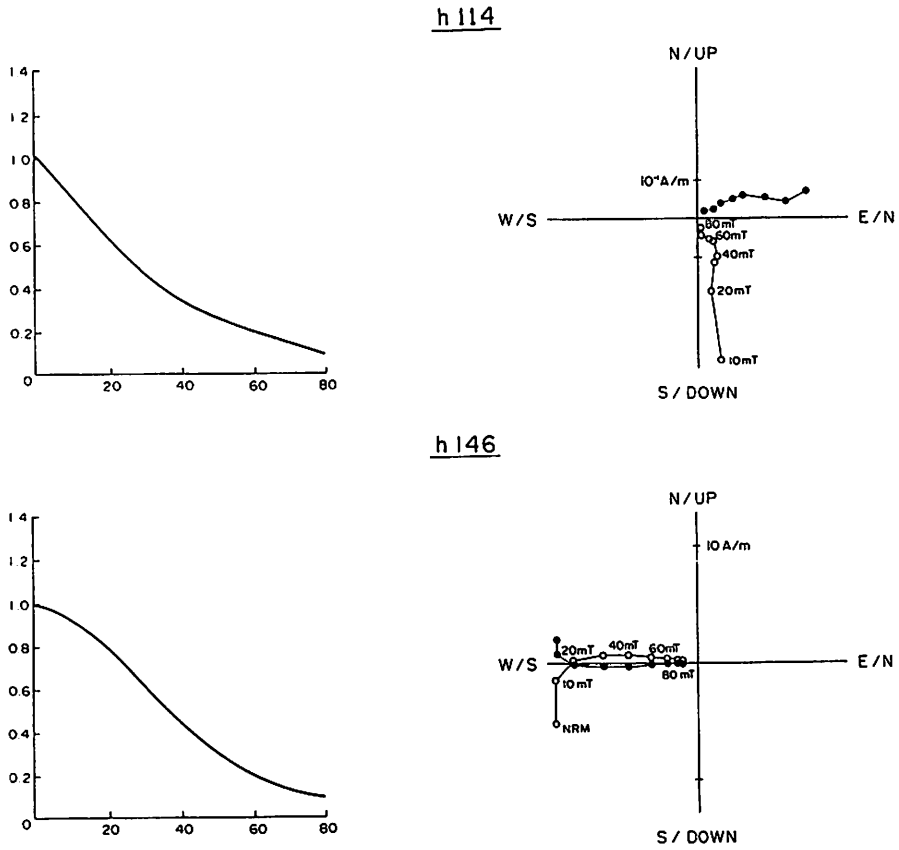


Fig. 5. (continued)

using Gregor et al.'s [1974] paleomagnetic data, but their analysis was inconclusive.

A prominent structural element, which may be significant for the internal deformation of the region is closely spaced horizontal right-lateral shear faults which cut throughout the region. This pattern implies inhomogeneous deformation which might be accomplished by rotation of the small blocks. If this is the case, paleomagnetic results can provide information on the amount and sense of the rotations, and from these the mechanism and amount of deformation can be inferred [Freund, 1974; Ron et al., 1984] and can then be tested against the predicted magnitude of deformation as derived from the "overlap" geometrical model (Figure 2).

## PALEOMAGNETIC STUDY

### Sampling and Laboratory Methods

Fifteen sites of Lower Cretaceous basalts, gabbro, and pyroclastic rocks (Table 1) were sampled in the Mount Hermon area (Figure 4). All samples, at least six from each of 13 sites were collected via field drilled cores using a sun compass to orient the samples. The accuracy of sample orientation is estimated at 2° for this method. Two sites of small gabbroic intrusions were sampled as oriented hand samples. Bedding attitude for all sites was carefully determined from the Jurassic and Lower Cretaceous sedimentary rocks. Remanent magnetization of all the samples was measured using a two-axis superconducting magnetometer. All specimens were progressively demagnetized by an alternating field (AF). The AF demagnetization was carried out inside the magnetometer in a field range from 5 to 80 mT, using a two-coil system. For comparison with the results of the AF treatment, one sample from each of the 15 sites was stepwise thermally demagnetized to 670°C. For each sample, a vector demagnetization (Figure 5), a normalized intensity curve ($J/J_o$, Figure 5) and a lower hemisphere stereonet plot were obtained in order to assess the magnetic

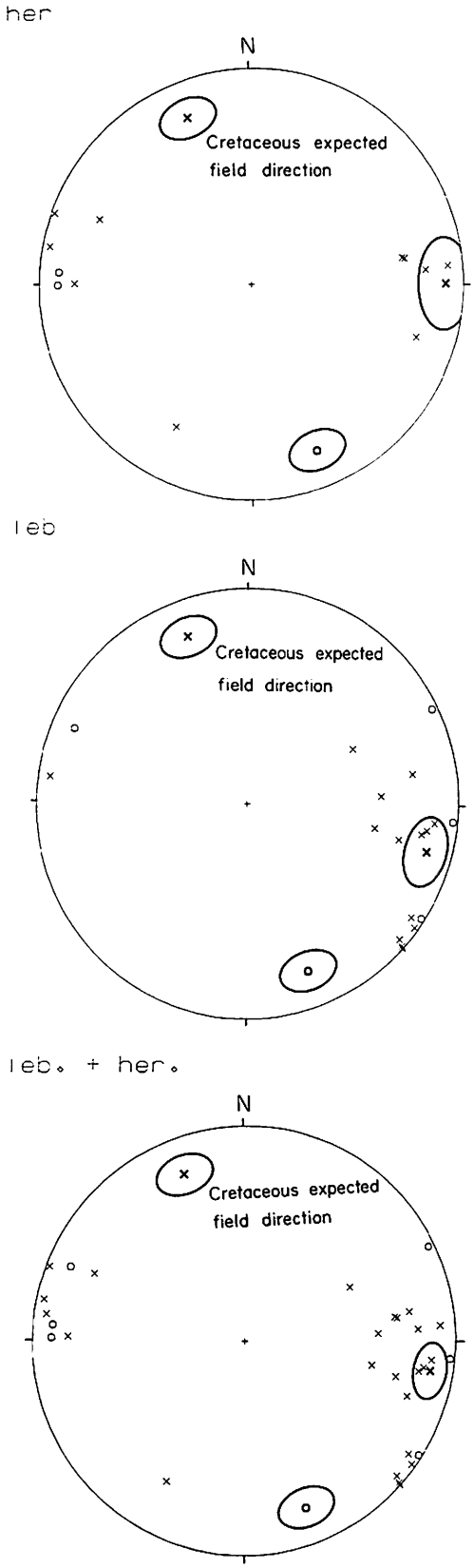


behavior. As a result, all samples from two sites (14, 15) were judged to be unstable and were excluded from further study.

About 90% of the samples show two components of magnetization; a low to moderate coercivity component is usually removed by AF demagnetization at a peak field of 20-30 mT or at a temperature of 300°C. This component is most likely a viscous remanent magnetization (VRM) which may have been induced by the recent field or may have been acquired during exposure of the rocks, probably in the Late Cenozoic time. The stable and characteristic magnetization components of each sample were isolated using Kirschvink's [1980] method.

## Analysis and Results

Site means were calculated using Fisher statistics [Fisher, 1953] and plotted on lower hemisphere stereonet (Figure 6a, Table 1). This data set which came east of the transform (the Arabian plate margin) was compared to the paleomagnetic data set of Gregor et al [1974]. Gregor et al.'s [1974] data came from west of the transform (the Sinai-Israel plate margin) and were obtained from rocks of the same age, 60-100 km northwest of the Hermon area (Table 2, Figure 6b). The two data sets show both normal and reverse polarity (Figure 6c) and are, statistically, the same type of data (Table 3) and therefore considered as one data group (Figure 6c). The data set thus defines the average direction of magnetization of Lower Cretaceous rocks from the deformed plate margins next to the Yammuneh fault segment of the Dead Sea transform.

The mean direction of magnetization was compared to the expected field direction for the Cretaceous of stable Africa

Fig. 6. (Opposite) Lower hemisphere stereographic projection of site mean directions of paleomagnetic vectors of Lower Cretaceous rocks: (a) Mount Hermon, (b) Mount Lebanon and (c) from Mounts Hermon and Lebanon together. The two antipodal ovals are the expected Cretaceous field direction of magnetization with the 95% confidence area about the mean. Open circles are of negative (up) inclination and crosses are of positive (down) inclination.

TABLE 2. Compilation of Paleomagnetic Data, Lebanon

| Site | N | Inc., deg. | Dec., deg. | $\alpha_{95}$° | K |
|---|---|---|---|---|---|
| 132 - 138a | 7 | 22.0 | 80.0 | 13.5 | 21 |
| 139 - 144 | 7 | 15.3 | 98.4 | 14.0 | 24 |
| 145 - 150 | 6 | -2.5 | 95.0 | 8.8 | 59 |
| 222 - 228 | 5 | 11.8 | 95.8 | 22.0 | 13 |
| 229 - 235 | 7 | 43.6 | 62.8 | 17.2 | 13 |
| 237 - 292 | 6 | 38.7 | 100.6 | 8.1 | 69 |
| 243 - 245 | 4 | 36.9 | 86.8 | 19.5 | 23 |
| 248 - 254 | 6 | 27.4 | 103.1 | 35.5 | 5 |
| 279 - 290 | 11 | 17.5 | 99.8 | 5.1 | 81 |
| 120 - 124 | 5 | 4.6 | 130.9 | 18.8 | 18 |
| 125 - 131 | 7 | -1.8 | 122.7 | 11.5 | 29 |
| 181 - 184 | 4 | 2.0 | 125.8 | 5.2 | 314 |
| 212 - 217 | 5 | -11.8 | 292.6 | 29.0 | 8 |
| 270 - 275 | 6 | 1.2 | 131.8 | 10.0 | 46 |
| 291 - 297 | 5 | 6.5 | 124.0 | 15.0 | 27 |
| 298 - 306 | 8 | 6.4 | 277.4 | 6.7 | 69 |
| 307 - 315 | 7 | 3.1 | 63.1 | 20.1 | 10 |
| 322 - 328 | 7 | 0.2 | 132.1 | 9.6 | 40 |

Source: Gregor et al. [1974], site numbers as in reference; for location, see reference. N, number of samples; inc., inclination; dec., declination; $\alpha_{95}$, radius of 95% confidence in deg; K, precision parameters.

as calculated by Ron et al. [1984] using various references (Table 3). The mean was also compared to Ron and Baer's [1987] data which were obtained from rocks of the same age in southern Israel (Table 3). Since the African reference directions were obtained from paleomagnetic poles of large age span (both Lower and Upper Cretaceous), the rotation and flattening were calculated using the southern Israel data [Ron and Baer, 1987] as a reference. The rotation and flattening were calculated using Beck's [1980] method as corrected by Demarest [1983].

TABLE 3. Results of Paleomagnetic Data

| Location | N | Inc., deg. | Dec., deg. | $\alpha_{95}$° | K |
|---|---|---|---|---|---|
| Lebanon* | 18 | 13.3 | 104.7 | 10.4 | 10.0 |
| Hermon† | 12 | 9.2 | 90.7 | 13.3 | 9.3 |
| Lebanon and Hermon | 30 | 11.7 | 99.1 | 8.3 | 9.4 |
| Ramon†† | 28 | 11.7 | 340.1 | 7.3 | 13.3 |
| Cretaceous (expected) | 5 | 17.6 | 338.3 | 9.1 | 103.1 |

N, number of site * or poles; inc., inclination; dec., declination; $\alpha_{95}$, radius of 95% confidence in deg; K, precision parameters. The reference poles for the Cretaceous (expected) are in the work by Ron et al. [1984].

*Gregor et al. [1974].

†This study.

††Ron and Baer [1987].

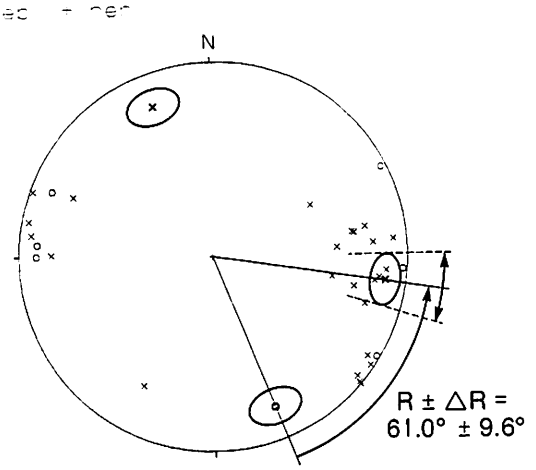


Fig. 7. Lower hemisphere stereographic projection of all-sites mean directions of paleomagnetic vectors of Lower Cretaceous rocks from the Lebanon and Mount Hermon area showing the sense and magnitude of rotation.

The results show a significant counter-clockwise (CCW) rotation of R±ΔR=61.Ø°±9.6° and a significant flattening of F±ΔF= 23.4° ±17.2° (Figure 7).

## Interpretation

The CCW rotation can be interpreted either as the rotation of two coherent microplates [Gregor et al., 1974] or as the result of internal rigid deformation by simultaneous strike-slip faulting and block rotation [Freund, 1974; Ron et al., 1984; Wells and Coe, 1985, and others].

There is no structural or tectonic evidence to support rigid plate rotation of the area in question; on the contrary, the plate margins are highly deformed by sets of east-west trending right-lateral faults (Figure 3). It is suggested that the deformation of the plate margins is accommodated by right-lateral strike-slip displacement and CCW rotation of the blocks between the faults by as much as 61°. Restoration of the right-lateral faults by the amount of rotation from east-west orientation will orient them to their inferred original NW trend. Figure 8 shows the mechanism and schematic fault geometry of the deformed plate margins. It is important to note that the rotation of 61° is a value obtained from a rather large area (Figure 3) and, therefore, demonstrates a regional average value.

However, the detailed picture is certainly more complex, since the deformation is not perfectly homogeneous. This may also assist us to understand the low value of K. The dispersion of the data is higher than expected by secular variation (SV); nevertheless, it is believed that the SV of the geomagnetic field is fully represented because the age of the rocks covers a long time span, and they show both normal and reverse polarity (Table 1) and have been collected from a large geographical area. It seems likely that a differential amount of rotation contributed to the data dispersion. The measured inclination is significantly shallower than that expected. The fact that this shallow inclination has also been reported by Van Dongen et al. [1967] and by Gregor et al. [1974] from rocks of the same age does not support any ambiguity in the structural correction. There is also no tectonic evidence to support the northward translation of this region as a single microplate, since geological formations of early Mesozoic age are continuous from Sinai and southern Israel into Lebanon and Syria. Furthermore, inclinations obtained from Lower Cretaceous rocks match the expected in southern Israel (Table 3). The shallow inclination is most likely the consequence of rotation about a slightly inclined axis.

Rotation about an inclined axis can be the result of displacement along strike-slip faults with oblique reverse components and simultaneous faulting and folding or the consequence of subsequent regional uplift which probably took place in the early Pliocene or later.

## DISCUSSION

Given the azimuth of the restraining fault bend and the direction of the relative plate slip vector, the geometrical model (Figure 2) predicts the width of the deformed zone. Combined with the observed amount of tectonic rotation, the magnitude of the shortening can also be predicted in respect to the plate slip vector. The assessment of these two parameters may show if the deformation of the plate margins indeed accommodates the 1Ø5 km left-lateral displacement along the Ø3Ø° trending restraining bend of the Dead Sea transform.

The width of the deformed zone is calculated perpendicular to the Yammuneh segment which strikes Ø3Ø° when the plate

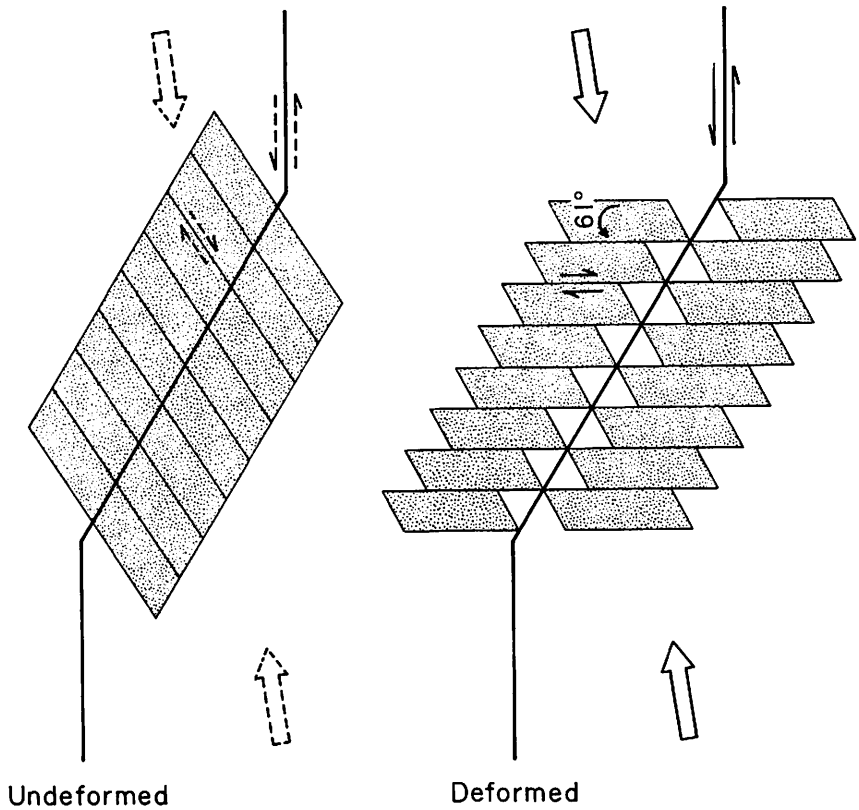


Fig. 8. Conceptual geometrical reconstruction of faulting and rotation of the investigated area (a) before fault slip and (b) after fault slip.

slip vector strikes 355° [Garfunkel, 1981; Joffe and Garfunkel, 1981] and the lateral displacement along the transform is 105 km [Freund et al, 1970]. Using (1), the predicted width is 55 km. The actual width of the zone defined by the Mount Lebanon, Beka'a valley, and Mount Hermon, perpendicular to the Yammuneh, is also approximately 55-60 km [Dubertret, 1955; Renouard, 1955; Beydoun, 1977]. The western boundary of the deformed zone is considered as the Mediterranean passive margin and the eastern boundary as the SE flank of the Hermon and Anti-Lebanon folds. Recently, Roperch and Bonhommet [1986] investigated the paleomagnetism of Miocene volcanic rocks 15-20 km east of Mount Hermon. They concluded that no tectonic rotation and deformation had occurred in this area since 20 Ma. This observation places a constraint on the maximum limit of the eastern boundary of the deformed zone and thus confines the maximum width of the zone of deformation to be circa 60 km.

The magnitude of the deformation accommodated by the E-W right-lateral strike-slip faulting and the 61° CCW rotation of the blocks between the faults can be calculated using simple geometrical relations [Ron et al., 1984; Garfunkel and Ron, 1985]. The deformation along a given line with an initial length, lo, and a final length, l, is

$$\lambda = lo/l = \sin(\alpha-\delta)/\sin\alpha \qquad (2)$$

where $\alpha$ is the initial angle between the faults and the line of deformation and $\delta$ is the angle of rotation (positive when counterclockwise), assuming rigid block rotation. If blocks are internally deformed, $\lambda$ will be underestimated. The values of deformation obtained using this method are shown in Table 4. The degree of shortening is then defined as $1/\lambda$.

The error in $1/\lambda$ is based on the uncertainty in the tectonic rotation R of $\Delta R=9.6°$. The calculated values of deformation imply that shortening of a given

TABLE 4. Calculated Magnitude Deformation

| Azimuth of Ref. Line | Initial Length | Final Length, $1/\lambda$ |
|---|---|---|
| 354°, parallel to plate slip vector | 1.0 | $0.5^{+0.10}_{-0.11}$ |
| 025°, parallel to Yammuneh segment | 1.0 | $1.0^{+0.12}_{-0.14}$ |
| 055° | 1.0 | $2.0^{+0.17}_{-0.18}$ |

See text for explanation.

line parallel to the slip vector is presently its half initial length, as predicted by the model (Figure 2) and that there is no deformation parallel to the Yammuneh (Figure 2). By using this method, the three axes of strain, maximum shortening, and maximum elongation and the axis of no strain have been calculated to construct the strain ellipse. Figure 9 demonstrates the strain ellipse of the deformation, obtained by strike-slip faulting and block rotation. In this reconstruction the line of no deformation is parallel to the transform plate boundary, the line of maximum shortening coincides with the direction of the plate slip vector, and the axis of maximum elongation is 61° clockwise off the axis of maximum shortening (Table 4, Figure 9).

The approximately 20% uncertainty in the magnitude of shortening allows for deformation accommodated by other mechanisms such as folding and tectonic stylolitization [Hancock and Atyia, 1979]. It appears that all these are probably minor deformational processes, whereas regional shear and block rotation about a slightly inclined axis constitute the major process accommodating deformation along the plate margins.

Nur et al. [1986] show that the amount of fault rotation permissible under a stationary stress field is limited to a maximum of 45° if blocks are defined by parallel fault sets. Thus block rotations larger than 40°-45° require more than one set of accompanying faults to accommodate the block rotation. Garfunkel [1981] and Joffe and Garfunkel [1987] show that the difference between the older (late Miocene) eular pole of the Sinai-Israel subplate and the younger (Pliocene to Recent) is no more than 5°. Furthermore, the irregular geometry of the northern Dead Sea transform implies that transverse compression has always been important along this section and, consequently, implies that the regional stress field, when considering the deformation of the plate margin, is stationary. Therefore structural analysis of fault geometry in the area may reveal that the right-lateral strike-slip faults are actually composed of two sets of faults: one older set trending E-W and a second younger set trending NW. If the seismicity in the plate margins [Rotstein and Arieh, 1986] is the manifestation of continuing deformation processes, then fault plane solutions of earthquakes on secondary faults will show right-lateral displacement along NW orienting faults. This type of current tectonic deformation has been recently observed and suggested by Nicholson et al. [1986] within the southern California.

## SUMMARY

The present study predicts and suggests a deformational mechanism for the plate margin adjacent to the restraining bend of transform faults by using first-order geometrical and kinematic considerations. The faults from kinematic and paleomagnetic data strongly support the idea that the regional shear is accommodated by secondary faulting and rigid block rotation.

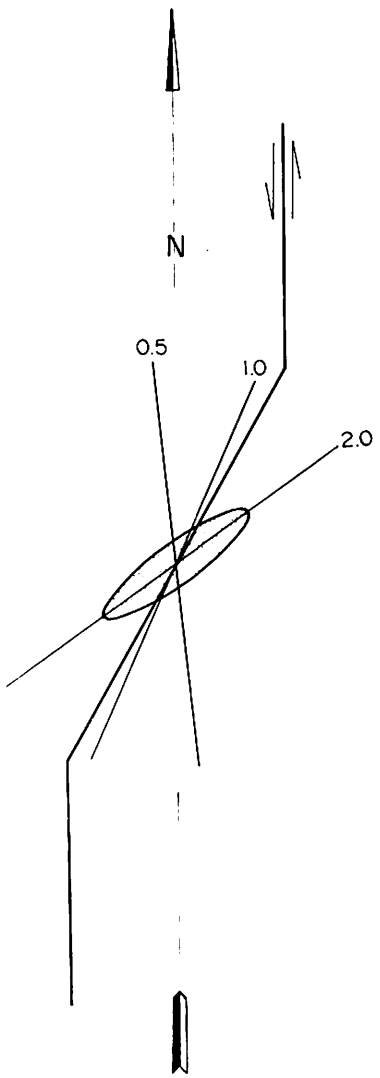


Fig. 9. The strain ellipse as calculated and reconstructed from the rotational data. The axis of maximum shortening is parallel to the direction of the plate slip vector and the line of no deformation is subparallel to the transform plate boundary.

It also suggests that the magnitude of deformation is directly controlled by the geometry of the restraining bend and the cumulative displacement along the transform fault. The predicted parameters of deformation can be tested using geological, structural and paleomagnetic data.

Acknowledgments. This project was initiated with support from the U.S.-Israel Binational Science Foundation, Grant 2155, and from the Geodynamics Program of the National Aeronautics and Space Administration, 1982-1983. This article benefited from helpful and sometimes challenging comments by Craig Nicholson, Sam Joffe, Amos Nur, and an anonymous reviewer. Mrs. D. Artzi typed the manuscript and improved its style.

REFERENCES

Beck, M. E., Jr., Paleomagnetic record of plate margin tectonic processes along the western edge of North America, J. Geophys, Res., 85, 7115-7131, 1980.

Beydoun, Z. R., Petroleum prospects of Lebanon, Bull. Am. Assoc. Petrol. Geol., 61, 43-64, 1977.

Demarest, H. H., Jr., Error analysis for the determination of tectonic rotation from paleomagnetic data, J. Geophys. Res., 88, 4321-4328, 1983.

Dubertret, M. L., Carte geologique du Liban, scale 1:50,000, Naqure, Bent Jabil, Tyr-Nabatiye and Marjayoung, Beirut, Ministry Public Works, 51 pp., 1955.

Fisher, R. A., Dispersion on a sphere, Proc. R. Soc. London, Ser A, 217, 295-305, 1953.

Freund, R., Kinematics of transform and transcurrent faults, Tectonophysics, 21, 93-134, 1974.

Freund, R., and D. H. Tarling, Preliminary Mesozoic paleomagnetic results from Israel and inferences for microplate structure in the Lebanon. Tectonophysics, 60, 189-205, 1979.

Freund, R., Z. Garfunkel, I. Zak, H. Goldberg, T. Weissbrod and B. Derin, The shear along the Dead Sea Rift, Philos, Trans. R. Soc. London, Series A, 267, 107-130, 1970.

Garfunkel, Z. Internal structure of the Dead Sea leaky transform (rift) in relation to plate kinematics, Tectonophysics, 80, (1-4), 84-108, 1981.

Garfunkel, Z. and H. Ron, Block rotation and deformation by strike slip faults, The properties of a type of macroscopic discontinuous deformation, J. Geophys. Res., 90, 8589-8602, 1985.

Garfunkel, Z., I. Zak and R. Freund, Active faulting in the Dead Sea Rift, Tectonophysics, 80 (1-4), 1-26, 1981.

Gregor, C. B., S. Mertzman, A. E. M. Narin and J. Negendank, Paleomagnetism of some Mesozoic and Cenozoic volcanic rocks from the Lebanon, Tectonophysics, 21, 375-395, 1974.

Hancock, P. L. and M. S. Atyia, Tectonic significance of the mesofractures systems associated with the Lebanese segment of the Dead Sea Transform fault, J. Struct. Geol., 1, 143-153, 1979.

Joffe, S. and A. Garfunkel, Plate kinematics of the circum Red Sea--A re-evaluation, Tectonophysics, in press, 1987.

Kirschvink, J. L., The least-squares line and plane and the analysis of paleomagnetic data, Geophys., J. R. Astron. Soc., 62, 699-718.

Kosloff, D., Numerical simulations of tectonic processes in southern California, Geophys. J. R. Astron. Soc., 51, 487-501, 1977

Mor, D., B. Land and G. Steinitz, The K-Ar age of the Mesozoic volcanism on the southeastern flank of Mount Hermon, Geol. Surv. Isr., Rep. GSI/36/84, 8 pp., 1984.

Nicholson, C., L. Seeber, P. Williams and L. R. Sykes, Seismic evidence for conjugate slip and block rotation within the San Andreas fault system, southern California, Tectonics, 5, 629-648, 1986.

Nur, A., H. Ron and O. Scotti, Fault mechanic and the kinematics of block rotation, Geology, 14, 746-749, 1986.

Renouard, G., Oil prospects of Lebanon, Am. Assoc. Pet. Geol. Bull., 39, 2125-2169, 1955.

Ron, H. and G. Baer, Paleomagnetism of Lower Cretaceous rocks from southern Israel, Paper presented at Israel Geological Society Annual Meeting, Mizpe Ramon, April, 1987.

Ron, H., R. Freund, Z. Garfunkel and A. Nur, Block rotation by strike slip faulting: Structural and paleomagnetic evidence, J. Geophys. Res., 89, 6256-6270, 1984.

Roperch, P. and N. Bonhommet, Paleomagnetism of Miocene volcanism from south Syria, J. Geophys., 59, 98-102, 1986.

Rotstein, Y. and E. Arieh, Tectonic implications of recent micro-earthquake data from Israel and adjacent areas, Earth Planet. Sci. Lett., 78, 237-244, 1986.

Segall, P. and D. Pollard, Mechanics of discontinuous faults, J. Geophys. Res., 85, 4337-4350, 1980.

Tiberghien, V., Le champ de la pesanteur au Liban et ses interpretations, Pubs. Tech. Sci., 26, 193 pp., Ecole Super. d'Ing. Beyrouth, Beiruit, Lebanon, 1974.

Van Dongen, G. P., R. Van Der Voo and Th. Raven, Paleomagnetic research in the central Lebanon mountains and in the Tartous area (Syria), Tectonophysics, 4, 35-53, 1967.

Wells, E. R. and R. S. Coe, Paleomagnetism and geology of Eocene volcanic rocks of southwest Washington, Implications for mechanism of tectonic rotation, J. Geophys. Res., 90, 1925-1947, 1985.

H. Ron, The Institute for Petroleum Research and Geophysics, P.O. Box 2286, Holon 58120, Israel.

(Received February 13, 1987;
revised May 11, 1987;
accepted May 22, 1987.)